Structure of quantum supercooled liquids

Gopika Krishnan * and Upendra Harbola
Department of Inorganic and Physical Chemistry, Indian Institute of Science, Bangalore 560012, India

(Received 10 October 2023; accepted 20 December 2023; published 16 January 2024)

Supercooled liquids show a drastic slowdown in the dynamics with decreasing temperature, while their structure remains similar to that of normal liquids. In this paper, the structural features in a quantum supercooled liquid are explored in terms of cages defined using the Voronoi polyhedra and characterized in terms of their volumes and geometries. The cage volume fluctuations are sensitive to the quantum effects, and decrease as the glass transition is approached by varying the quantumness. This is in contrast to the classical case where the volumes are insensitive to temperature variations as one approaches the transition. The cage geometry becomes more spherical upon increasing quantumness from zero, pushing the system closer to the glass transition. The cage geometry is found to be significantly correlated with asymmetry in the position uncertainty of the caged particle in the strongly quantum regime.

DOI: 10.1103/PhysRevE.109.014115

I. INTRODUCTION

The dynamics of a liquid slows down drastically upon supercooling, leading to the phenomenon of a glass transition due to confinement of the particles, or "caging," by their neighbors. It is not well understood what structural changes, if any, accompany the phenomenon of a glass transition. The liquid structure, as analyzed in terms of a two-point structural correlation, the structure factor, or equivalently, the radial distribution function, does not show significant changes as one approaches the glass transition. It is therefore desirable to identify structural features that may exhibit significant variations upon supercooling and possibly indicate a thermodynamic origin of the glass transition, which is currently a focus of much research. Several works have studied the presence of locally favored structures and tried to identify the correlation of slow dynamics with local structural parameters such as tetrahedrality and packing efficiency [1–3] and more complex quantities derived from machine learning approaches [4], and diverging correlation lengths associated with higher-order structural correlations [5].

In this paper, we study the microscopic structural properties of a quantum supercooled liquid. It has been recognized in recent years that quantum effects may bring in interesting changes in the behavior of liquids at low temperatures. Some examples include the linear temperature dependence of the specific heat in glasses at low temperatures (<1 K) in contrast to the expected cubic temperature dependence in crystals [6–9], suppression of the glass-transition temperature of low T_g materials [10,11], and anomalous behavior in the diffusion coefficients of H_2 and D_2 at low temperatures in nanoporous substrates [12–14]. The observations in Refs. [10–14] suggest that the quantum effects can either slow down or make the dynamics faster, indicating a nonmonotonous (reentrant) behavior in the glassy nature as one scans through the whole regime of quantumness from weak ($\Lambda <$ particle size) to strong ($\Lambda >$ particle size), where $\Lambda = \sqrt{\frac{\hbar^2\beta}{2m}}$ is the thermal de Broglie wavelength of the particle of mass m, and β is the inverse temperature. This reentrant behavior has been observed in quantum simulations in simple model systems [15,16].

We employ path-integral molecular dynamics simulations to account for the quantum effects. We particularly focus on the structure of cages in the regimes of weak and strong quantumness. The reentrant behavior allows one to define two types of liquids, with an intervening glass transition: one where caging potential effects are relatively important (a weak quantum regime), and the other where tunneling effects are significant (a strong quantum regime). Our study indicates that the cage geometries and their size distributions depend on supercooling and can be a static indicator of the reentrant behavior of the glass transition in quantum liquids. We further show that in a strongly quantum regime, the liquid structure around the cages having significantly different geometries, may show qualitative differences, although the radial distribution function of the liquid shows no interesting feature upon supercooling by varying the quantumness. The cage geometry is found to be correlated with the asymmetry in the quantum uncertainty in the position of the caged particle. This correlation increases with the quantumness.

II. SIMULATION MODEL AND METHODS

We consider a three-dimensional glass forming liquid [17] consisting of two species A and B, in a ratio of 80:20. The system consists of 1000 particles with a number density 1.206. The interaction between two particles, α and β, is given by the Lennard-Jones potential,

$$V_{\alpha\beta}(r) = 4\epsilon_{\alpha\beta}\left\{\left(\frac{\sigma_{\alpha\beta}}{r}\right)^{12} - \left(\frac{\sigma_{\alpha\beta}}{r}\right)^{6}\right\}, \quad (1)$$

*gopikak@iisc.ac.in

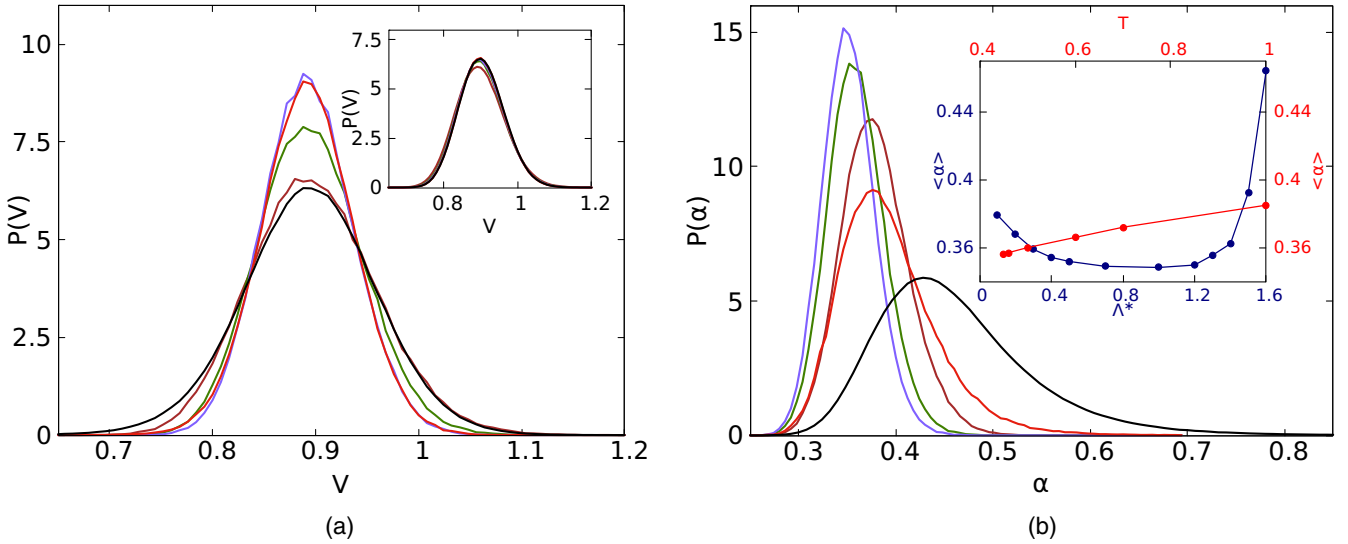

FIG. 1. The probability distribution of (a) volumes (V) and (b) asphericities (α) of the cages for $\Lambda^* = 0.1$ (brown), 0.3 (green), 0.5 (purple), 1.5 (red), and 1.6 (black). The inset in (a) shows the distribution of cage volumes in the classical case, for $T = 1.0$ (brown), 0.7 (green), 0.6 (purple), 0.5 (red), and 0.46 (black). The inset in (b) shows the variation of average asphericity ($\langle\alpha\rangle$) as a function of Λ^* (blue) for the quantum case and temperature (red) for the classical case.

where r is the distance between two particles, and $\sigma_{\alpha\beta}$ and $\epsilon_{\alpha\beta}$ are the effective size and the interaction energy, respectively. The distance is in units of σ_{AA}. The mass m is set to unity for both species. The length scales and timescales are in units of σ_{AA} and $\tau = \sqrt{m\sigma_{AA}^2/\epsilon_{AA}}$, respectively. This model is well known to show a dynamic slowdown typically observed going closer to the glass transition in the classical case [18,19].

The path-integral formalism incorporates quantum effects using a mapping between a quantum particle and a classical ring polymer [20] with P beads. Path-integral molecular dynamics [21,22] simulations are carried out starting from equilibrium configurations from classical simulations at the desired temperature. The quantumness of the system is varied by manipulating $\hbar$. If the de Broglie wavelength is small compared to the classical size (σ) of the particle, the quantum effects are insignificant in the system. As the de Broglie wavelength becomes comparable to the particle size, quantum effects start to play an important role in dictating the properties of the system. The limit $\hbar \to 0$ gives the classical limit. Results presented are for the major component of the system (A-type species) at a fixed temperature, $T = 1.0$, and different $\Lambda^* = \Lambda/\sigma_{AA}$ obtained by varying $\hbar$. Classically, at this temperature, the system is in the normal liquid regime showing fast (relaxation time $\tau_\alpha \sim \tau$) exponential relaxation. In the quantum case, however, even at $T = 1.0$, it is possible to push the system to the supercooled state by increasing Λ^* from zero, leading to a marked increase in the relaxation times ($\sim$3 orders of magnitude) of the system (see Table I), and back to the liquid state, by further increasing Λ^* to values greater than the particle size as shown in Refs. [15,23], resulting in the reentrant behavior in the dynamics as a function of quantumness.

TABLE I. The relaxation time (τ), average values of cage volumes ($\langle V\rangle$), and asphericities ($\langle\alpha\rangle$) for different values of quantumness.

Λ^*	τ	$\langle V\rangle$	$\langle\alpha\rangle$
0.1	1.79	0.8983	0.3791
0.2	5.8	0.8968	0.3678
0.3	36	0.8953	0.3599
0.4	664	0.8942	0.3542
0.5	6745	0.8929	0.3518
1.3	174	0.8908	0.3554
1.4	58	0.8909	0.3623
1.5	4.26	0.8921	0.3925
1.6	0.77	0.8937	0.4541

III. STRUCTURAL PROPERTIES OF CAGES

The cage of a particle is defined by the volume exclusively available for the particle by considering configurations of nearest neighbors. This is done using the Voronoi polyhedra [24,25] of the center of mass (c.m.) of ring polymers, which is a classical-like degree of freedom of the quantum particle, and is an estimate of the average position of the quantum particle. In a disordered system, the Voronoi polyhedra, defined as the space closer to its central atom than to any other, give us some insights about the variations in the three-dimensional (3D) local environment of particles than the radial distribution function, which is an average quantity [26]. The Voronoi polyhedra divide the total volume to volumes exclusively available for each particle, giving a measure of local density around each particle. Each snapshot of the system configuration is analyzed in terms of the Voronoi polyhedra properties, volume (V) and asphericity (α), to characterize the cages.

The distribution of cage volumes for different values of quantumness is shown in Fig. 1(a). Although the average volume of cages remains unaffected, fluctuations in the volume distribution are significantly affected as quantumness is

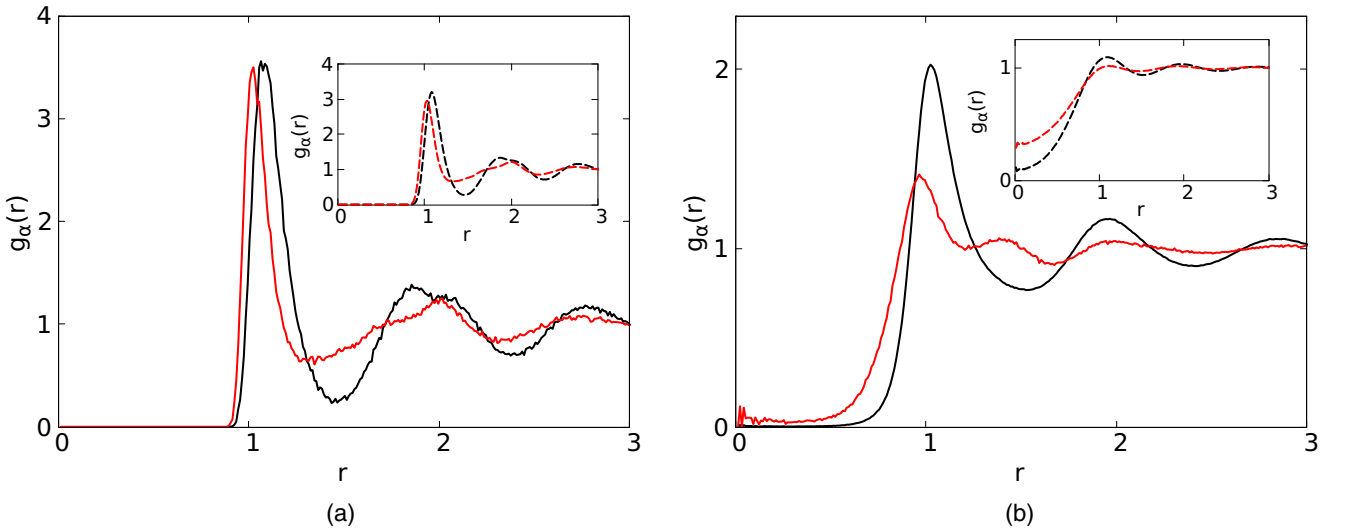

FIG. 2. The radial distribution function for the c.m. of the ring polymer, for particles with lowest (black curves) and highest (red curves) 10% of asphericities for (a) $\Lambda^* = 0.1$ and (b) $\Lambda^* = 1.6$. The insets in (a) and (b) show the corresponding radial distribution function for the beads.

varied. It is observed that the fluctuations decrease as one approaches the transition point; the system becomes more homogeneous in terms of the cage volumes as one goes deeper into the supercooled state. This indicates that in the weak quantum regime, the local density variations decrease with increasing quantumness, although the relaxation timescale of density fluctuations is known to increase with increasing quantum effects [27]. In the strong quantum regime, the fluctuation in volume increases with increasing quantumness, while the timescale of density relaxation decreases. In contrast, in the classical case, the local density fluctuations are found to be insensitive to the temperature variations [see the inset of Fig. 1(a)] [28], although their relaxation time increases drastically upon lowering the temperature [18]. Thus in the weak quantum region, the liquid becomes more homogeneous in terms of density fluctuations as the quantumness is increased, while a reverse trend is seen in the strong quantum regime.

We next analyze the geometries of the cages in terms of their asphericities, defined as the ratio $\alpha = \frac{S^3}{36\pi V^2} - 1$, where S is the total surface area and V is the volume of the polyhedron, respectively. This provides an estimate of how close the polyhedron is to a sphere ($\alpha = 0$). A truncated octahedron, a rhombic dodecahedron, and a cube have $\alpha = 0.33$, 0.35, and 0.91, respectively. A comparison of the distribution of asphericities of polyhedra as a function of Λ^* is shown in Fig. 1(b). Increasing quantumness in the moderate quantum regime leads to shifting of the average asphericity ($\langle\alpha\rangle$) to lower values. The distribution becomes more homogeneous upon supercooling. Thus, going towards the glass transition, cages tend to become more spherical. Similar behavior is also observed in the classical case, where the glass transition is approached by decreasing the temperature. Going towards the stronger quantum regime, the asphericities become broadly distributed with a larger average value. A comparison of $\langle\alpha\rangle$ for the classical and quantum system is shown in the inset of Fig. 1(b), which clearly shows that cages become more spherical as the transition point is approached both in the classical and quantum liquids. However, on the stronger quantum regime, this gives way to an increasing trend of $\langle\alpha\rangle$ with increasing Λ^* while the liquid becomes less glassy as the relaxation time decreases. Thus, the average asphericity values reflect the reentrant behavior of the dynamics observed in the system.

Does a change in the geometry of a cage cause any significant change in the local liquid structure? In order to explore this, we consider the particles with cages of highest and lowest (10%) α values in the distribution, and study the liquid structure around these particles, in terms of the radial distribution function $g_\alpha(r)$ of the c.m. of ring polymers. This is shown in Fig. 2 for two Λ^* values. In the weak quantum system, there are no qualitative differences in the local structure around particles with different cage geometries. However, in the strong quantum regime, there are significant differences in the

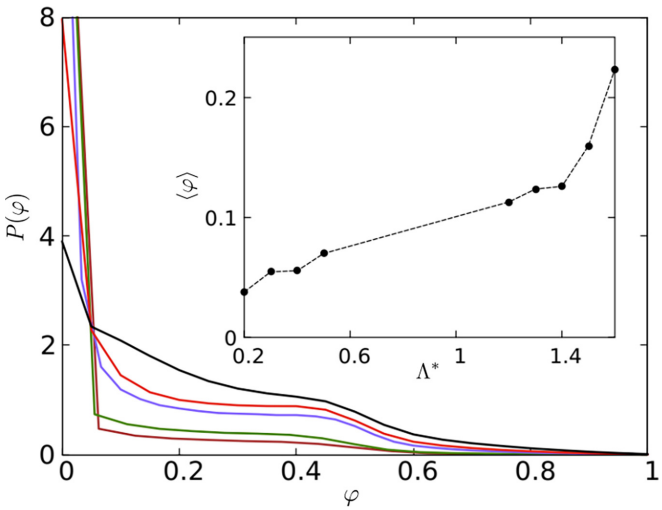

FIG. 3. Tunneling fraction for $\Lambda^* = 0.2$ (brown), 0.4 (blue), 1.3 (green), 1.5 (red), and 1.6 (black). The inset shows the average tunneling fraction ($\langle\varphi\rangle$) as a function of Λ^*.

TABLE II. The average tunneling fraction (φ) and the anisotropy of polymer shapes ($\mathcal{R}$).

Λ^*	$\langle\varphi\rangle$	$\langle\mathcal{R}\rangle$
0.1	0.0224	0.0008
0.2	0.038	0.0148
0.3	0.054	0.0181
0.4	0.0558	0.0204
0.5	0.08929	0.0214
1.3	0.125	0.00305
1.4	0.143	0.0350
1.5	0.159	0.0454
1.6	0.226	0.0675

structure around the particles of cages of different asphericities as shown in Fig. 2(b). The sharper first maximum in $g_\alpha(r)$ for regions around particles with low α indicates that these regions are more structured. On the other hand, in the high asphericity regions, the nearest neighbors are closer, as implied by the additional peak arising in the intermediate $r \approx 1.4\sigma_{AA}$ for high α values. Note that for strong quantumness, the local structure obtained in terms of bead radial distribution around the cages with different asphericity shows qualitatively different behavior and predicts a significant nonzero probability for particles to be found even at zero distance, which is more pronounced in the neighborhood of particles with larger asphericity cages. This is a consequence of the position uncertainty in quantum liquids. For distances $r > \sigma_{AA}$, the structure is almost flat, resembling the structure of a gaseous system.

IV. QUANTIFYING TUNNELING IN QUANTUM LIQUIDS

The reentrant behavior in the dynamics of the system is a result of predominant tunneling in the strong quantum regime [16]. The spread of the beads of the ring polymer with respect to the c.m. (average position of the quantum particle) is an indicator of the position uncertainty of the quantum particle [15,29]. The greater the spread of the beads, the larger is the position uncertainty of the quantum particle, indicating a higher propensity of tunneling. As discussed in Sec. III, the Voronoi volume gives an estimate of the confinement of the quantum particle by its neighbors, or the cage. Thus, the cage

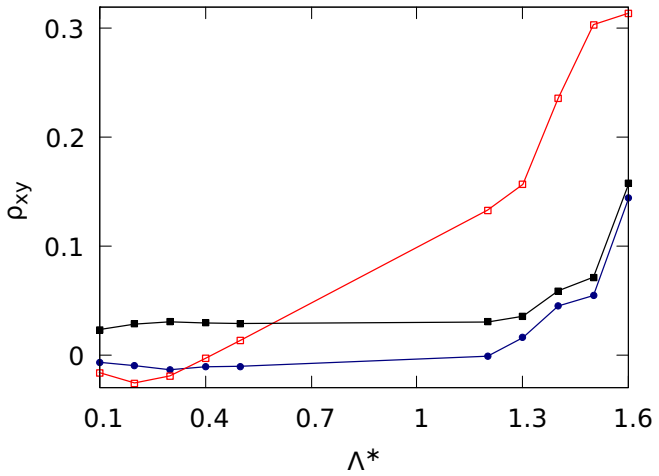

FIG. 5. The correlation coefficients for $\alpha - \phi$ (blue solid circles), $\alpha - \mathcal{R}$ (red open squares), and $\mathcal{R} - \varphi$ (black solid squares) as a function of Λ^*.

defined this way can be interpreted as the classical potential in which the particle is confined, while the beads outside the cages denote the weight of the probability of the particle to be outside this potential and thus is a measure of the tunneling. Hence, we define tunneling as the fraction of beads outside the Voronoi volume defined for the quantum particle. The tunneling fraction (φ) for different Λ^* is shown in Fig. 3. For low values of quantumness the tunneling fraction is low, since the uncertainty in particle position is smaller than the cage size. As quantumness increases, the position uncertainty grows, leading to a higher probability of finding the particle outside its cage. The variation of average tunneling fraction ($\langle\varphi\rangle$) as a function of quantumness is shown in the inset of Fig. 3 and in Table II. For the highest quantumness studied, the value is ∼22%. The tunneling fraction of around 12% is significant enough to bring in the liquidlike behavior in the system, although this will depend on the strength of the confining potential.

Given the geometries of the cages are significantly heterogeneous in the strong quantum regime, it is a relevant question to ask whether the shapes of the ring polymer reflect a similar heterogeneity and whether the two heterogeneities are correlated. Anisotropy in the shape of a ring polymer is analyzed in

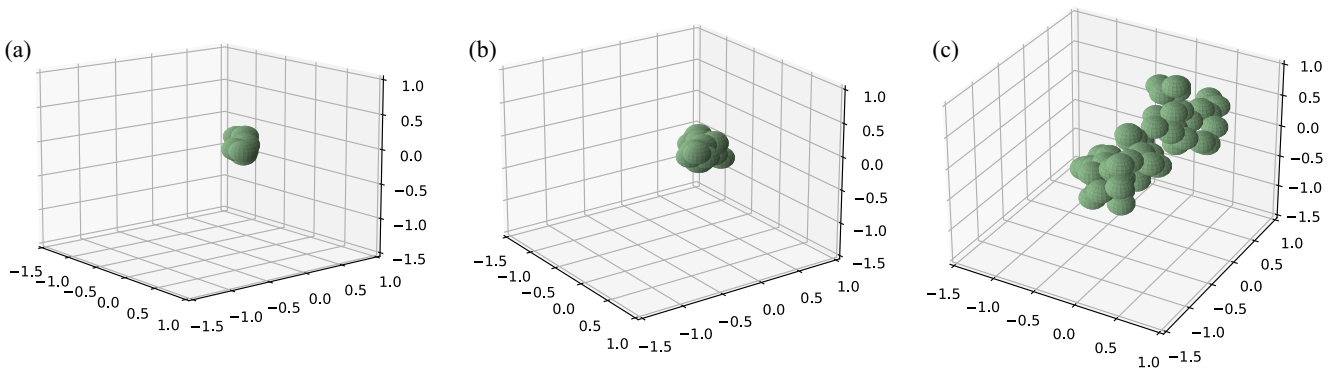

FIG. 4. The position of beads with respect to the center of mass for (a) $\Lambda^* = 0.2$, (b) $\Lambda^* = 0.4$, and (c) $\Lambda^* = 1.6$.

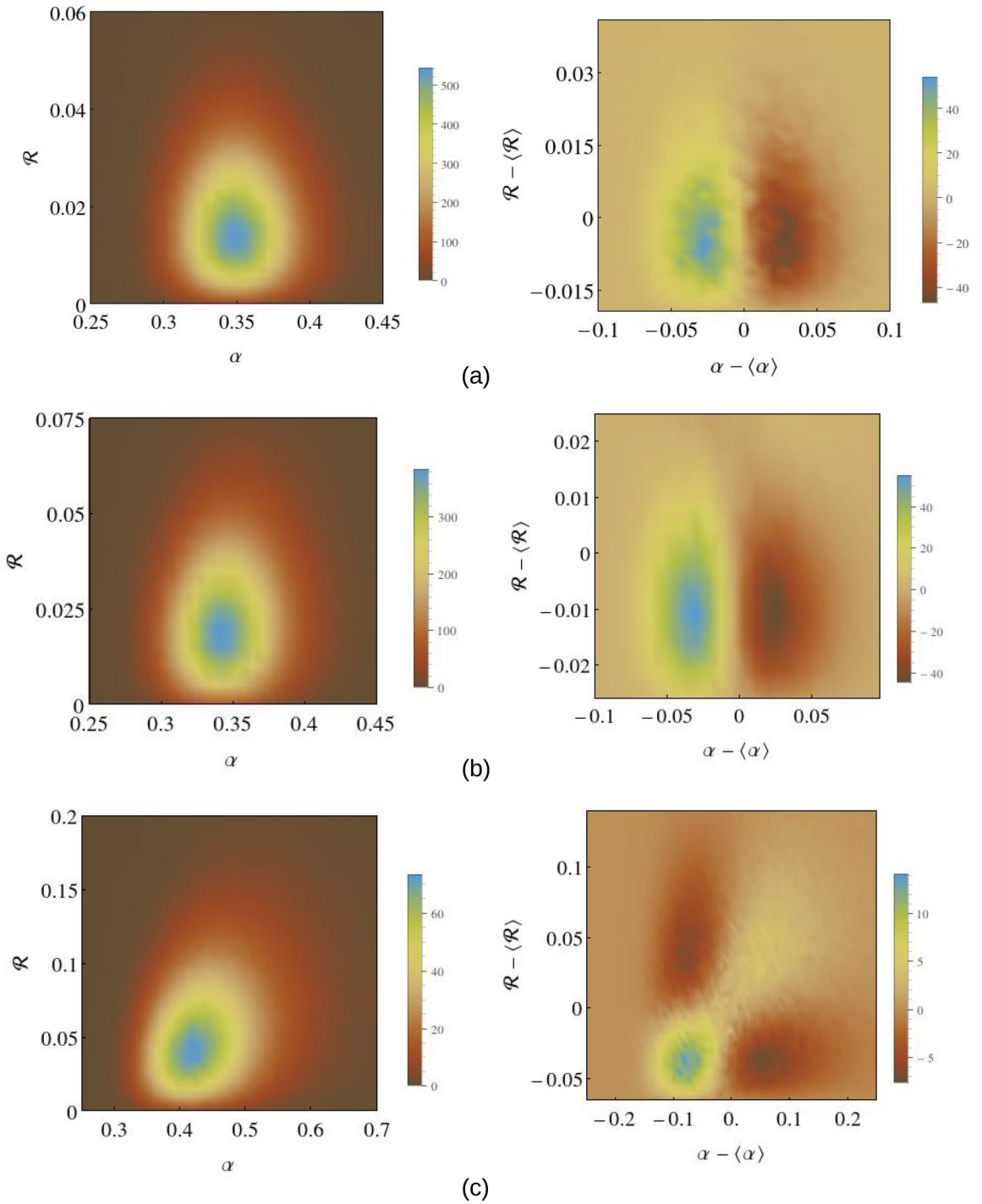

FIG. 6. Joint probability distribution of the variables α and $\mathcal{R}$ (left panel), and the quantity $P(\alpha, \mathcal{R}) - P(\alpha)P(\mathcal{R})$ (right panel) for (a) $\Lambda^* = 0.4$, (b) $\Lambda^* = 1.2$, and (c) $\Lambda^* = 1.6$.

terms of the instantaneous difference in the radius of gyration, $R_{g\mu} = \sqrt{\frac{1}{P}\sum_{i=1}^{P}(\mu_i - \mu_{cm})^2}$, $\mu \in x, y, z$, along the three axes and quantified by the parameter

$$\mathcal{R} = \frac{1}{3}\sum_{\mu}\sum_{\nu\neq\mu}|R_{g\mu} - R_{g\nu}|. \tag{2}$$

Averaging over the ensemble, it is observed that $\mathcal{R}$ increases systematically with increasing quantumness. The values are presented in Table II and the typical shapes of the ring-polymer in the weak, moderate and strong quantum regime are shown in Fig. 4.

To identify the possible correlations between the tunneling fraction, asphericity, and the anisotropy in the polymer shape, we calculate the correlation coefficient between each pair of variables, defined by [30]

$$\rho_{xy} = \frac{1}{N_s}\frac{\sum_{i=1}^{N_s}(x_i - \langle x\rangle)(y_i - \langle y\rangle)}{\sigma_x\sigma_y}, \tag{3}$$

where $\langle \cdots \rangle$ denotes the average over the sample, σ_x and σ_y are the standard deviations of variables x and y, respectively, and N_s is the number of observations. In the weak quantum regime, the variables show poor correlation. However, in the strong quantum regime, the variables α and $\mathcal{R}$ show significant positive correlations as seen from Fig. 5. This is also evident from the joint distribution $P(\alpha, \mathcal{R})$ which is symmetric about the mean values [see Fig. 6(a)] and becomes increasingly distorted in the strong quantum regime [Fig. 6(c)]. A measure of interdependence of the two variables is identified by analyzing the quantity $\Delta = P(\alpha, \mathcal{R}) - P(\alpha)P(\mathcal{R})$ and is depicted in the right-hand panel of Fig. 6 for three different Λ^*. For the weak quantum regime, Δ is antisymmetric with respect to $\langle \alpha \rangle$, implying that the two sides show an opposing correlation between the variables leading to a small value of $\rho_{\alpha\mathcal{R}}$. In the strong quantum regime, a large positive correlation is seen to arise from the $(\alpha, \mathcal{R})$ regions lower than the average values, leading to the net positive value of $\rho_{\alpha\mathcal{R}}$.

V. CONCLUSIONS

The Voronoi polyhedra carry more structural information than the average structure calculated by the radial distribution function, and give insights into the local structure around the particles in the system. It is observed that the average cage volume is insensitive to the quantum effects. But quantumness does affect the fluctuations in the volume distribution. Nearing the glass transition by increasing the quantumness, the system becomes more homogeneous in terms of the cage volumes. This is in contrast to the classical case, where nearing the glass transition by changing temperature does not have a significant effect on the volume distribution. The cage geometries, understood in terms of the asphericities, show that the cages become more spherical as one approaches the glass transition. In the strong quantum regime, where the system moves towards the liquid state as the quantumness is increased, a broad distribution of asphericities is observed. The structures around particles with high and low asphericities are considerably different in the strongly quantum regime: Regions with higher asphericities have nearest neighbors closer as compared to the regions of low asphericity. The tunneling fraction increases systematically with increasing quantumness. The shape anisotropy of the ring polymer increases with increasing quantum effects, indicating the polymer being stretched in one of the directions as tunneling increases. The cage geometry and polymer shape anisotropy are seen to be significantly (positively) correlated in the strong quantum regime. Thus, as the tunneling facilitates the escape of particles from their cages, which become more anisotropic, the ring polymers also acquire an anisotropic shape in the strong quantum regime.

ACKNOWLEDGMENTS

G.K. acknowledges the support from Council of Scientific and Industrial Research, India. U.H. acknowledges Science and Engineering Research Board (SERB) of India for support under Grant No. CRG/2020/0011100.

[1] H. Tanaka, T. Kawasaki, H. Shintani, and K. Watanabe, Critical-like behaviour of glass-forming liquids, Nat. Mater. **9**, 324 (2010).

[2] A. Malins, J. Eggers, C. P. Royall, S. R. Williams, and H. Tanaka, Identification of long-lived clusters and their link to slow dynamics in a model glass former, J. Chem. Phys. **138**, 12A535 (2013).

[3] S. Marín-Aguilar, H. H. Wensink, G. Foffi, and F. Smallenburg, Tetrahedrality dictates dynamics in hard sphere mixtures, Phys. Rev. Lett. **124**, 208005 (2020).

[4] E. Boattini, S. Marín-Aguilar, S. Mitra, G. Foffi, F. Smallenburg, and L. Filion, Autonomously revealing hidden local structures in supercooled liquids, Nat. Commun. **11**, 5479 (2020).

[5] G. Biroli, J.-P. Bouchaud, K. Miyazaki, and D. R. Reichman, Inhomogeneous mode-coupling theory and growing dynamic length in supercooled liquids, Phys. Rev. Lett. **97**, 195701 (2006).

[6] R. C. Zeller and R. O. Pohl, Thermal conductivity and specific heat of noncrystalline solids, Phys. Rev. B **4**, 2029 (1971).

[7] P. W. Anderson, B. I. Halperin, and C. M. Varma, Anomalous low-temperature thermal properties of glasses and spin glasses, Philos. Mag. **25**, 1 (1972).

[8] T. Pérez-Castañeda, C. Rodríguez-Tinoco, J. Rodríguez-Viejo, and M. A. Ramos, Suppression of tunneling two-level systems in ultrastable glasses of indomethacin, Proc. Natl. Acad. Sci. USA **111**, 11275 (2014).

[9] D. Khomenko, C. Scalliet, L. Berthier, D. R. Reichman, and F. Zamponi, Depletion of two-level systems in ultrastable computer-generated glasses, Phys. Rev. Lett. **124**, 225901 (2020).

[10] V. N. Novikov and A. P. Sokolov, Role of quantum effects in the glass transition, Phys. Rev. Lett. **110**, 065701 (2013).

[11] V. N. Novikov and A. P. Sokolov, Quantum effects in dynamics of water and other liquids of light molecules, Eur. Phys. J. E **40**, 57 (2017).

[12] R. Kumar, J. R. Schmidt, and J. L. Skinner, Hydrogen bonding definitions and dynamics in liquid water, J. Chem. Phys. **126**, 204107 (2007).

[13] T. X. Nguyen, H. Jobic, and S. K. Bhatia, Microscopic observation of kinetic molecular sieving of hydrogen isotopes in a nanoporous material, Phys. Rev. Lett. **105**, 085901 (2010).

[14] C. I. Contescu, H. Zhang, R. J. Olsen, E. Mamontov, J. R. Morris, and N. C. Gallego, Isotope effect on adsorbed quantum phases: Diffusion of H_2 and D_2 in nanoporous carbon, Phys. Rev. Lett. **110**, 236102 (2013).

[15] T. E. Markland, J. A. Morrone, B. J. Berne, K. Miyazaki, E. Rabani, and D. R. Reichman, Quantum fluctuations can promote or inhibit glass formation, Nat. Phys. **7**, 134 (2011).

[16] T. E. Markland, J. A. Morrone, K. Miyazaki, B. J. Berne, D. R. Reichman, and E. Rabani, Theory and simulations of quantum glass forming liquids, J. Chem. Phys. **136**, 074511 (2012).

[17] W. Kob and H. C. Andersen, Scaling behavior in the β-relaxation regime of a supercooled

Lennard-Jones mixture, Phys. Rev. Lett. **73**, 1376 (1994).

[18] W. Kob and H. C. Andersen, Testing mode-coupling theory for a supercooled binary Lennard-Jones mixture. II. Intermediate scattering function and dynamic susceptibility, Phys. Rev. E **52**, 4134 (1995).

[19] W. Kob and H. C. Andersen, Testing mode-coupling theory for a supercooled binary Lennard-Jones mixture I. The van Hove correlation function, Phys. Rev. E **51**, 4626 (1995).

[20] D. Chandler and P. G. Wolynes, Exploiting the isomorphism between quantum theory and classical statistical mechanics of polyatomic fluids, J. Chem. Phys. **74**, 4078 (1981).

[21] S. Plimpton, Fast parallel algorithms for short-range molecular dynamics, J. Comput. Phys. **117**, 1 (1995).

[22] R. Freitas, M. Asta, and V. V. Bulatov, Quantum effects on dislocation motion from ring-polymer molecular dynamics, npj Comput. Mater. **4**, 55 (2018).

[23] A. Das, G. Krishnan, E. Rabani, and U. Harbola, Tagged particle dynamics in supercooled quantum liquids, Phys. Rev. E **105**, 054136 (2022).

[24] G. Voronoi, Nouvelles applications des paramètres continus à la theorie des formes quadratiques, J. Reine Angew. Math. **133**, 97 (1907).

[25] C. H. Rycroft, VORO++: A three-dimensional Voronoi cell library in C++, Chaos **19**(4), 041111 (2009).

[26] J. C. G. Montoro and J. L. F. Abascal, The Voronoi polyhedra as tools for structure determination in simple disordered systems, J. Phys. Chem. **97**, 4211 (1993).

[27] G. Krishnan and U. Harbola, Dynamics of transient cages in a model 2D supercooled liquid, Int. J. Mod. Phys. B **36**, 2250065 (2022).

[28] S. Bernini, F. Puosi, and D. Leporini, Weak links between fast mobility and local structure in molecular and atomic liquids, J. Chem. Phys. **142**, 124504 (2015).

[29] T. F. Miller, Isomorphic classical molecular dynamics model for an excess electron in a supercritical fluid, J. Chem. Phys. **129**, 194502 (2008).

[30] D. Freedman, R. Pisani, and R. Purves, *Statistics (International Student Edition)*, 4th ed. (W. W. Norton, New York, 2007).